

Modulo- $(2^{2n} + 1)$ Arithmetic via Two Parallel n -bit Residue Channels

1st Ghassem Jaberipur
dept. of Computer Engineering
Chosun University
Gwangju, Republic of Korea
Jaberipur@chosun.ac.kr

2nd Bardia Nadimi
dept. of Computer Science and Engineering
University of South Florida
Tampa, Florida, United States
bnadimi@usf.edu

3rd Jeong-A Lee
dept. of Computer Engineering
Chosun University
Gwangju, Republic of Korea
jalee@chosun.ac.kr

Abstract—Augmenting the balanced residue number system moduli-set $\{m_1 = 2^n, m_2 = 2^n - 1, m_3 = 2^n + 1\}$, with the co-prime modulo $m_4 = 2^{2n} + 1$, increases the dynamic range (DR) by around 70%. The Mersenne form of product $m_2 m_3 m_4 = 2^{4n} - 1$, in the moduli-set $\{m_1, m_2, m_3, m_4\}$, leads to a very efficient reverse converter, based on the New Chinese remainder theorem. However, the double bit-width of the m_4 residue channel is counter-productive and jeopardizes the speed balance in $\{m_1, m_2, m_3\}$. Therefore, we decompose m_4 to two complex-number n -bit moduli $2^n \pm \sqrt{-1}$, which preserves the DR and the co-primality across the augmented moduli set. The required forward modulo- $(2^{2n} + 1)$ to moduli- $(2^n \pm \sqrt{-1})$ conversion, and the reverse are immediate and cost-free. The proposed unified moduli- $(2^n \pm \sqrt{-1})$ adder and multiplier, are tested and synthesized using Spartan 7S100 FPGA. The 6-bit look-up tables (LUT), therein, promote the LUT realizations of adders and multipliers, for $n = 5$, where the DR equals $2^{25} - 2^5$. However, the undertaken experiments show that to cover all the 32-bit numbers, the power-of-two channel m_1 can be as wide as 12 bits with no harm to the speed balance across the five moduli. The results also show that the moduli- $(2^5 \pm \sqrt{-1})$ add and multiply operations are advantageous vs. moduli- $(2^5 \pm 1)$ in speed, cost, and energy measures and collectively better than those of modulo- $(2^{10} + 1)$.

Index Terms—Residue Number Systems, FPGA Realization, Complex-Number Moduli, Modular Adders and Multipliers

I. INTRODUCTION

Residue number systems (RNS) are the basis for the arithmetic units in several digital systems, such as cryptosystems [1], digital signal processing [2], image processing [3], and recently varieties of neural network hardware accelerators [4]–[13]. Fast low power/cost modular addition and multiplication, via speed-balanced residue channels with small bit-width, are the desirable and essential properties for the working RNS moduli set. As well, are the reasonably efficient forward residue generation and reverse multi-residue to binary conversion.

The classic moduli set $T = \{2^n, 2^n - 1, 2^n + 1\}$ is quite popular and has been of utmost utility for decades. The range

of uniquely representable numbers, often called the dynamic range (DR), in T equals $[0, 2^{3n} - 2^n)$. It covers up to 18-bit integers in $[0, 262080)$, for small $n \leq 6$. Such DR satisfies the working range in many applications, especially convolutional and deep neural networks (CNN and DNN).

The corresponding modular adders and multipliers, operating on at most 6-bit operands, are quite fast on different technological platforms. In particular, they are suitable for realization on field programmable gate arrays (FPGA) with 6-bit look-up tables (LUT) [14].

Another important property of T is the realization of efficient residue generators and reverse conversion circuitry. Implementation of the latter, via the New Chinese remainder theorem (NCRT) [15] consists of a $2n$ -bit carry-save adder (CSA) and a modulo- $(2^{2n} - 1)$ addition unit.

There are other CNN and DNN hardware accelerators that use RNS with other possibly higher moduli than those of the aforementioned 6-bit T . For example,

- 1) The three works in [5], [9], [16] use the moduli set $\{31, 32, 63\}$, to compute the results of their activation function, maximum pooling unit, and the processing element units.
- 2) The moduli set $\{8, 63, 127\}$, is used in [11] for computing the results of the convolutions or matrix products followed by the bias adjustment.
- 3) The work of [13], is based on $\{31, 32, 32, 29, 35\}$ and $\{511, 512, 513\}$, which offers an RNS-based convolution layer for the inferring stage.
- 4) A new CNN architecture is proposed in [17], in which convolution layers have a hardware implementation on FPGA using the RNS arithmetic with special moduli set $\{31, 128, 511\}$.

The moduli set, in all the above examples 1) to 4) are imbalanced, where the maximum bit-widths are 6, 7, 10, 9, respectively. However, the required DR can be covered via the moduli set $F = \{2^n, 2^n - 1, 2^n + 1, 2^{2n} + 1\}$, with smaller bit-widths $n \in \{4, 4, 6, 5\}$, respectively. This 4-moduli set F shares the property of simple reverse conversion of T , since the final operation in the corresponding NCRT reverse converter is a modulo- $(2^{4n} - 1)$ addition. However, the modulo- $(2^{2n} + 1)$ Residue channel for F is not speed-balanced with the other

Jaberipur's research was supported by the Brain Pool program, funded by the Ministry of Science and ICT, through the National Research Foundation of Korea (RS-2023-00263909), and Lee's research is supported by Basic Science Research Program funded by the Ministry of Education through the National Research Foundation of Korea (NRF-2020R111A3063857).

three moduli. Therefore, in this work, we present the new balanced adaptive moduli set $F_c = \{2^{n+p}, 2^n - 1, 2^n + 1, 2^n - j, 2^n + j\}$, where $j = \sqrt{-1}$, and the DR is exactly equal to that of F , since $(2^n - j)(2^n + j) = 2^{2n} + 1$. Moreover, we design the required moduli- $(2^n \pm j)$ addition and multiplication schemes for LUT realization on Spartan 7S100 FPGA platform. Since the real [imaginary] parts of moduli- $(2^n \pm j)$ residues are represented in $(n + 1)$ -bit stored borrow [carry] format, our experiments are centered on $n = 5$, for best use of the 6-bit LUTs of the working FPGA.

The choice of adaptive moduli set is due to the fact that the speed of Spartan 7S100 modulo- 2^{n+p} adders and multipliers are in balance with other moduli of F_c , for $p \leq n$, per the results of our experiments. Our contributions in this work are:

- n -bit realization of modulo- $(2^{2n} + 1)$ RNS arithmetic, via complex-number moduli.
- Efficient realizations, for $n = 5$, on FPGA with 6-bit LUTs.
- Taking advantage of the high performance of power-of-two modular adders and multipliers on the utilized FPGA, for setting up an adaptive moduli set.

The remaining sections of this paper discuss the following subjects. A foundational background on general RNS in Section II, followed by an in-depth examination of residue generation, adders, and multipliers for modulo- $(2^n \pm j)$ in Section III, which concludes with the critical discussion on the reverse conversion of modulo- $(2^n \pm j)$ residues to modulo- $(2^{2n} + 1)$. In Section IV, we present a comparative assessment of the newly introduced complex moduli in contrast to modulo- $(2^{2n} + 1)$, along with a comparison of the proposed moduli-set to other moduli sets employed in earlier DNN hardware accelerator studies. The paper concludes in Section V with a summary of findings and potential directions for future research.

II. A BACKGROUND ON GENERAL RNS

A typical residue number system is characterized by k co-prime moduli $R = \{m_1, \dots, m_k\}$, where the DR is usually denoted by $M = m_1 \times \dots \times m_k$. A binary number $X \in [0, M)$ is represented in R , as $(x_1 \dots, x_k)$, where $x_i = |X|_{m_i}$ (i.e., the remainder of integer division X/m_i), for $1 \leq i \leq k$. Execution of an arithmetic operation $Z = X \otimes Y$, where $\otimes \in \{+, \times, -\}$, and $X, Y, Z \in [0, M)$, is distributed within k parallel computational residue channels (one per each modulo in R), such that $Z = (z_1 \dots, z_k)$, and $z_i = |x_i \otimes y_i|_{m_i}$, for $1 \leq i \leq k$.

Other arithmetic operations such as division, comparison, and sign detection cannot be performed in parallel and generally require reverse conversion of the operands to binary, while there exist some shortcut methods (e.g., [18]).

There are three major reverse conversion schemes, based on the Chinese remainder theorem (CRT); namely, the plain CRT, New CRT (NCRT), and mixed radix. The NCRT, as in (1) is of particular interest in this work, since it simplifies the reverse conversion, where $M = 2^n(2^{p \times n} - 1)$, which is the case in the proposed F moduli set, for $p = 4$.

$$X = x_1 + m_1 \left| \sum_{i=1}^{k-1} \mu_i (x_{i+1} - x_i) \right|_{M_1}, \quad (1)$$

$$\mu_i = \left(\prod_{j=2}^i m_j \right) \left(\prod_{j=1}^i m_j \right)^{-1} \Big|_{\prod_{j=i+1}^k m_j}$$

III. MODULO- $(2^n \pm j)$ ARITHMETIC

Recalling the 4-moduli set F , that covers $5n$ -bit numbers $Z \in [0, 2^{5n} - 2^n)$, in this section, we provide for the forward convertor yielding $X = |Z|_{2^{2n}+1} \in [0, 2^{2n}]$, followed by modulo- $(2^n \pm j)$ residue $|X|_{2^n \pm j}$ generator, adder, multiplier, and reverse double residues $|X|_{2^n \pm j}$ -to- X convertor.

A. Modulo- $(2^n \pm j)$ residue generator

Let $Z = 2^{4n}Z_2 + 2^{2n}Z_1 + Z_0$, represents the $5n$ -bit numbers within the dynamic range of F , where $Z_2 = z_{5n-1} \dots z_{4n} \in [0, 2^n - 1]$, $Z_1 = z_{4n-1} \dots z_{2n} \in [0, 2^{2n} - 1]$, and $Z_0 = z_{2n-1} \dots z_0 \in [0, 2^{2n} - 1]$. It can be shown (See the Appendix) that $X = |Z|_{2^{2n}+1} \in [0, 2^{2n}]$ is representable as in (2), where $x_{2n} = 1 \rightarrow x_{2n-1} \dots x_0 = 0$.

$$X = x_{2n-1} \dots x_0 + \overline{x_{2n}} \quad (2)$$

Let $X = 2^n X_I + X_R + \overline{x_{2n}}$, where $X_R, X_I \in [0, 2^n)$. Therefore, the desired complex residues of X are obtained, as in (3), where $|2^n|_{2^n \pm j} = |2^n \pm j \mp j|_{2^n \pm j} = \mp j$. Note that this X -to- $|X|_{2^n \pm j}$ conversion, is immediate and cost-free.

$$|X|_{2^n \pm j} = X_R + \overline{x_{2n}} \mp j X_I \quad (3)$$

B. Modulo- $(2^n \pm j)$ adders

We design the required $|X + Y|_{2^n \pm j}$ adders with the practical assumption that one operand is always coming from the forward convertor as $|X|_{2^n \pm j} = X_R + \overline{x_{2n}} \mp j X_I$, per (3). The other operand is the accumulated modular sum, as the output of the modulo- $(2^n \pm j)$ adders. However, the generated carry bits c_{R_n} and c_{I_n} of the real and imaginary sums are transferred to the other part, since $|2^n c_{R_n}|_{2^n \pm j} = \mp j c_{R_n}$, and $|\mp j 2^n c_{I_n}|_{2^n \pm j} = |\mp j \times \mp j c_{I_n}|_{2^n \pm j} = -c_{I_n}$. Therefore, we assume stored borrow (carry) representation for the real (imaginary) part of the accumulated sum, as $|Y|_{2^n \pm j} = Y_R - b_y \mp j(Y_I + c_y)$, where $Y_R, Y_I \in [0, 2^n)$, and $b_y, c_y \in \{0, 1\}$. Consequently, $|S|_{2^n \pm j} = |X + Y|_{2^n \pm j}$ can be unfolded as in (4), where the following propositions are in order, with due justification to follow, for the second one.

- 1) $\overline{x_{2n}} - b_y = \overline{b_y x_{2n}} - b_y x_{2n}$,
- 2) $S_R, S_I' \in [0, 2^n)$, $c_s' = c_n + c_y x_{2n} = c_n \vee c_y x_{2n}$, and $b_s = c_n + b_y x_{2n} = c_n \vee b_y x_{2n}$, since $c_n x_{2n} = c_n x_{2n} = 0$.

The reason, for the latter, is that $x_{2n} = 1 \rightarrow X_R = X_I = 0 \rightarrow 2^n c_n + S_R = X_R + Y_R + \overline{b_y x_{2n}} = Y_R \rightarrow c_n = 0 \rightarrow c_s = c_y$, and $2^n c_n' + S_I' = X_I + Y_I + c_y \overline{x_{2n}} = Y_I \rightarrow c_n' = 0 \rightarrow b_s = b_y$.

- Derivation of $|S|_{2^n \pm j}$:

$$\begin{aligned}
|S|_{2^n \pm j} &= \\
|X_R + \overline{x_{2n}} \mp jX_I + Y_R - b_y \mp j(Y_I + c_y)|_{2^n \pm j} &= \\
|X_R + \overline{x_{2n}} + Y_R - b_y \mp j(X_I + Y_I + c_y)|_{2^n \pm j} &= \\
|(X_R + Y_R + \overline{b_y x_{2n}}) - b_y x_{2n} \mp & \\
j(X_I + Y_I + c_y \overline{x_{2n}}) \mp j c_y x_{2n}|_{2^n \pm j} &= \\
|(2^n c_n + S_R) - b_y x_{2n} \mp j(2^n c'_n + S_I) \mp j c_y x_{2n}|_{2^n \pm j} &= \\
|S_R - c'_n - b_y x_{2n} \mp j(S_I + c_n + c_y x_{2n})|_{2^n \pm j} &\rightarrow
\end{aligned}$$

$$\begin{aligned}
|S|_{2^n \pm j} &= S_R - b_S \mp j(S_I + c_S), \\
b_S &= c'_n \vee b_y x_{2n}, c_S = c_n \vee c_y x_{2n}
\end{aligned} \tag{4}$$

C. LUT realization of the modulo- $(2^n \mp j)$ adders

Recalling $|X|_{2^n \pm j} = X_R + \overline{x_{2n}} \mp jX_I$, and $|Y|_{2^n \pm j} = Y_R - b_y \mp j(Y_I + c_y)$, let $X_I = x_{2n-1} \cdots x_n$, $X_R = x_{n-1} \cdots x_0$, $Y_I = y_{2n-1} \cdots y_n$, and $Y_R = y_{n-1} \cdots y_0$. Therefore, the required $(2^{n+1} + 2) \times (2^n + 1)$ -bit LUTs are described as follows.

$$\begin{aligned}
2^n c_n + S_R &= LUT(X_R, Y_R, x_{2n}, b_y) = X_R + Y_R + \overline{b_y x_{2n}}, \\
2^n c'_n + S_I &= LUT(X_I, Y_I, x_{2n}, c_y) = X_I + Y_I + c_y \overline{x_{2n}}, \\
b_S &= \lfloor \frac{X_I + Y_I + c_y \overline{x_{2n}}}{2^n} \rfloor \vee b_y x_{2n}, \\
c_S &= \lfloor \frac{X_R + Y_R + \overline{b_y x_{2n}}}{2^n} \rfloor \vee c_y x_{2n}
\end{aligned}$$

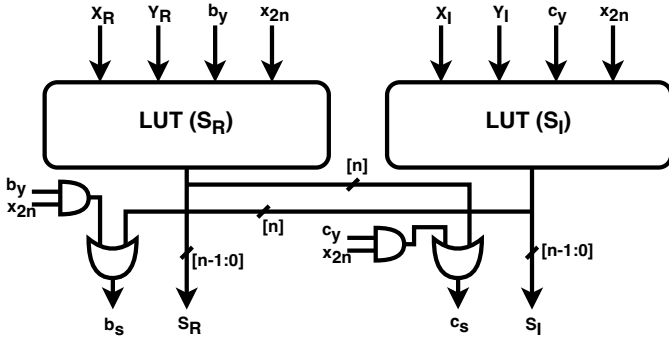


Fig. 1. Proposed complex-number modulo Adder diagram.

D. Modulo- $(2^n \pm j)$ multipliers

Let $X = x_{2n-1} \cdots x_0 + \overline{x_{2n}}$ and $Y = y_{2n-1} \cdots y_0 + \overline{y_{2n}}$ denote the multiplicand and multiplier, both as modulo- $(2^{2n} + 1)$ residues generated by F -to- $(2^{2n} + 1)$ convertor (see the Appendix). Therefore, recalling that $x_{2n} = 1 \rightarrow x_i = 0$, and $y_{2n} = 1 \rightarrow y_i = 0$, for $0 \leq i < 2n$, the corresponding modulo- $(2^n \pm j)$ residues are $|X|_{2^n \pm j} = \overline{x_{2n}} + X_R \mp jX_I = \overline{x_{2n}}(1 + X_R \mp jX_I)$, and $|Y|_{2^n \pm j} = \overline{y_{2n}} + Y_R \mp jY_I = \overline{y_{2n}}(1 + Y_R \mp jY_I)$. Consequently, $|X \times Y|_{2^n \pm j}$ is expressed as follows.

$$\begin{aligned}
|X \times Y|_{2^n \pm j} &= \\
|\overline{x_{2n}} \overline{y_{2n}} (1 + X_R \mp jX_I)(1 + Y_R \mp jY_I)|_{2^n \pm j} &= \\
\overline{x_{2n}} \overline{y_{2n}} |(1 + X_R)(1 + Y_R) \mp j(1 + X_R)Y_I \mp & \\
jX_I(1 + Y_R) - X_I \times Y_I|_{2^n \pm j} &
\end{aligned} \tag{5}$$

Let the four product expressions, within 5, be expressed as 1 to 4, below:

- 1) $(1 + X_R)(1 + Y_R) = 2^{2n}c + 2^n H_{RR} + L_{RR} \rightarrow |(1 + X_R)(1 + Y_R)|_{2^n \pm j} = |L_{RR} - c \mp jH_{RR}|_{2^n \pm j}$
- 2) $(1 + X_R)Y_I = 2^n H_{RI} + L_{RI} \rightarrow |(1 + X_R)Y_I|_{2^n \pm j} = |L_{RI} \mp jH_{RI}|$
- 3) $X_I(1 + Y_R) = 2^n H_{IR} + L_{IR} \rightarrow |X_I(1 + Y_R)|_{2^n \pm j} = |L_{IR} \mp jH_{IR}|$
- 4) $X_I \times Y_I = 2^n H_{II} + L_{II} \rightarrow 2^{2n} - 1 - X_I \times Y_I = 2^{2n} - 1 - (2^n H_{II} + L_{II}) = 2^n \overline{H_{II}} + \overline{L_{II}} \times | -X_I \times Y_I|_{2^n \pm j} = |2^{2n} + 1 - X_I \times Y_I|_{2^n \pm j} = |2 + 2^n \overline{H_{II}} + \overline{L_{II}}|_{2^n \pm j} \rightarrow | -X_I \times Y_I|_{2^n \pm j} = |2 + \overline{L_{II}} \mp j\overline{H_{II}}|_{2^n \pm j}$

Therefore,

$$\begin{aligned}
|X \times Y|_{2^n \pm j} &= \\
\overline{x_{2n}} \overline{y_{2n}} |L_{RR} - c \mp jH_{RR} \mp j(L_{RI} \mp jH_{RI}) \mp j(L_{IR} \mp jH_{IR}) & \\
+ 2 + \overline{L_{II}} \mp j\overline{H_{II}}|_{2^n \pm j} &= \overline{x_{2n}} \overline{y_{2n}} |L_{RR} - c + \overline{L_{II}} - H_{RI} - \\
H_{IR} + 2 \mp j(H_{RR} + L_{RI} + L_{IR} + \overline{H_{II}})|_{2^n \pm j} &
\end{aligned}$$

Given that $| -H_{RI} - H_{IR}|_{2^n \pm j} = |2(2^n \pm j) - H_{RI} - H_{IR}|_{2^n \pm j} = |\overline{H_{RI}} + \overline{H_{IR}} + 2 \pm 2j|_{2^n \pm j}$, further elaboration leads to:

$$\begin{aligned}
|X \times Y|_{2^n \pm j} &= |L_{RR} + \overline{L_{II}} + \overline{H_{RI}} + \overline{H_{IR}} + 1 - c + 3 \pm 2j \mp \\
j(\overline{H_{RR}} + L_{RI} + L_{IR} + \overline{H_{II}})|_{2^n \pm j} &= |L_{RR} + \overline{L_{II}} + \overline{H_{RI}} + \\
\overline{H_{IR}} + \overline{c} + 3 \mp j(H_{RR} + L_{RI} + L_{IR} + \overline{H_{II}} - 2)|_{2^n \pm j} &\rightarrow \\
|X \times Y|_{2^n \pm j} &= |R \mp jI|_{2^n \pm j}, \text{ where}
\end{aligned}$$

$$\begin{aligned}
R &= L_{RR} + \overline{L_{II}} + \overline{H_{RI}} + \overline{H_{IR}} + \overline{c} + 3, \\
I &= H_{RR} + L_{RI} + L_{IR} + \overline{H_{II}} - 2
\end{aligned} \tag{6}$$

E. LUT realization of $|X \times Y|_{2^n \pm j}$

The required LUTs for the four (H, L) pairs in 1) to 4), of Section III-D, are described as LUT_1 to LUT_4 , below.

$$\begin{aligned}
LUT_1((1 + X_R)(1 + Y_R)) &= 2^{2n}c + 2^n H_{RR} + L_{RR}. \\
LUT_2((1 + X_R)Y_I) &= 2^n H_{RI} + L_{RI}. \\
LUT_3(X_I(1 + Y_R)) &= 2^n H_{IR} + L_{IR}. \\
LUT_4(X_I \times Y_I) &= 2^n H_{II} + L_{II}.
\end{aligned}$$

Trusting $R - 3 = L_{RR} + \overline{L_{II}} + \overline{H_{RI}} + \overline{H_{IR}} + \overline{c}$ to a n -bit $(4; 2)$ compressor, leads to $|R - 3|_{2^n \pm j} = |2^n v_n + 2^n c_n + \hat{V} + \hat{U}|_{2^n \pm j} = |\hat{V} + \hat{U} \pm j(v_n + c_n)|_{2^n \pm j}$, where $\hat{V} = v_{n-1} \cdots v_1 0$, and $\hat{U} = u_{n-1} \cdots u_0$. Similar compression of $I + 2 + c_n + v_n = H_{RR} + L_{RI} + L_{IR} + \overline{H_{II}} + c_n + v_n$, results in $|I + 2 + c_n + v_n|_{2^n \pm j} = |2^n v'_n + 2^n c'_n + \hat{V}' + \hat{U}'|_{2^n \pm j} = |\hat{V}' + \hat{U}' \pm j(v'_n + c'_n)|_{2^n \pm j}$, where $\hat{V}' = v'_{n-1} \cdots v'_1 v'_0$, $\hat{U}' = u'_{n-1} \cdots u'_0$. Therefore,

TABLE I
(4; 2) COMPRESSORS FOR THE MULTIPLIER

(4; 2) compressors $6\Delta G$	L_{RR}	d_{n-1}	\dots	d_1	d_0	H_{RR}	e_{n-1}	\dots	e_1	e_0
	L_{II}	f_{n-1}	\dots	f_1	f_0	L_{RI}	h_{n-1}	\dots	c_1	c_0
	H_{RI}	l_{n-1}	\dots	l_1	l_0	L_{IR}	r_{n-1}	\dots	r_1	r_0
	H_{IR}	t_{n-1}	\dots	t_1	t_0	H_{II}	g_{n-1}	\dots	g_1	g_0
Carry-save adders $2\Delta G$	\hat{U}	u_{n-1}	\dots	u_1	u_0	\hat{U}'	u'_{n-1}	\dots	u'_1	u'_0
	$\hat{V} + \hat{v}'_n$	v_{n-1}	\dots	v_1	v_n	\hat{V}'	v'_{n-1}	\dots	v'_1	v'_0
					c'_n		$2^n - 2$		1	
										1
n -bit adders	W	w_{n-1}	\dots	w_1	w_0	W'	w'_{n-1}	\dots	w'_1	w'_0
	Z	z_{n-1}	\dots	z_1	z_0	Z'	z'_{n-1}	\dots	z'_1	z'_0
$ R \pm jI _{2^n \pm j}$	P_R	p_{n-1}	\dots	p_1	p_0	P_I	p'_{n-1}	\dots	p'_1	p'_0
					$-b_P$					c_P
										$\times \pm j$

$$\begin{aligned}
|R \mp jI|_{2^n \pm j} &= |\hat{V} + \hat{U} \mp j(v_n + c_n) + 3\mp \\
&\quad j(\hat{V}' + \hat{U}' \mp j(v'_n + c'_n) - 2 - c_n - v_n)|_{2^n \pm j} = \\
&= |\hat{V} + \hat{U} - v'_n - c'_n + 3\mp \\
&\quad j(\hat{V}' + \hat{U}' + 2^n - 2 - 2^n)|_{2^n \pm j} = \\
&= |\hat{V} + \hat{U} + 1 - v'_n + 1 - c'_n + 1\mp \\
&\quad j(\hat{V}' + \hat{U}' + 2^n - 2 \pm j)|_{2^n \pm j} =
\end{aligned}$$

$$\begin{aligned}
|\hat{V} + \hat{U} + \overline{v'_n} + \overline{c'_n} + 2 \mp j(\hat{V}' + \hat{U}' + 2^n - 2)|_{2^n \pm j} &\rightarrow \\
|R \mp jI|_{2^n \pm j} &= \\
|\hat{V} + \hat{U} + \overline{v'_n} + \overline{c'_n} + 2 \mp j(\hat{V}' + \hat{U}' + 2^n - 2)|_{2^n \pm j} &\quad (7)
\end{aligned}$$

Let $L_{RR} = \overline{d_{n-1}} \dots \overline{d_0}$, $H_{RR} = \overline{e_{n-1}} \dots \overline{e_0}$, $L_{II} = \overline{f_{n-1}} \dots \overline{f_0}$, $H_{II} = \overline{g_{n-1}} \dots \overline{g_0}$, $L_{RI} = \overline{h_{n-1}} \dots \overline{h_0}$, $H_{RI} = \overline{l_{n-1}} \dots \overline{l_0}$, $L_{IR} = \overline{r_{n-1}} \dots \overline{r_0}$, $H_{IR} = \overline{t_{n-1}} \dots \overline{t_0}$. The LUT realization of the n -bit adders that yield the product $P_R - b_P \mp j(P_I + c_P)$ are as follows.

$$\begin{aligned}
P_R &= LUT(W, Z) = |W + Z + 1|_{2^n}, c_P = \frac{W+Z+1}{2^n} \\
P_I &= LUT(W', Z') = |W' + Z'|_{2^n}, b_P = \frac{W'+Z'}{2^n}.
\end{aligned}$$

F. Immediate and cost-free Reverse moduli- $(2^n \pm j)$ to modulo- $(2^{2n} + 1)$ convertor

The reverse conversion task is meant to derive the $(2n + 1)$ -bit $S[P]$ from the two conjugate residues of the modulo- $(2^n \pm j)$ sum [product], such that $|S|_{2^n \pm j} = S_R - b_S \mp j(S_I + c_S)$ [$|P|_{2^n \pm j} = P_R - b_P \mp j(P_I + c_P)$].

The modulo- $(2^{2n} + 1)$ sum S can be expressed as $S = 2^n(s_I + c_s) + s_R - b_s$, which is easily verifiable. However, to obtain a clean-cut $(2n + 1)$ -bit result for S , we derive $S = |S|_{2^{2n} + 1}$, as follows, where similar undertakings apply to P .

$$\begin{aligned}
S &= |2^n(s_I + c_s) + s_R - b_s|_{2^{2n} + 1} = \\
&= |2^{2n} + 2^n s_I + s_R + 2^n c_s + \overline{b_s}|_{2^{2n} + 1}, \text{ which can be obtained via} \\
&\text{a sparse modulo-}(2^{2n} + 1) \text{ adder, where the main operand is} \\
&\text{the } (2n + 1)\text{-bit } 2^{2n} + 2^n s_I + s_R \text{ and the sparse one contains} \\
&\text{only two bits in positions } 0(\overline{b_s}), \text{ and } n(c_s).
\end{aligned}$$

However, since this result is used in a further reverse conversion, along the moduli- $(2^n \pm 1)$ and the power-of-two modulo, it can be used as $S = 2^n(s_I + c_s) + s_R - b_s$, where no cost nor

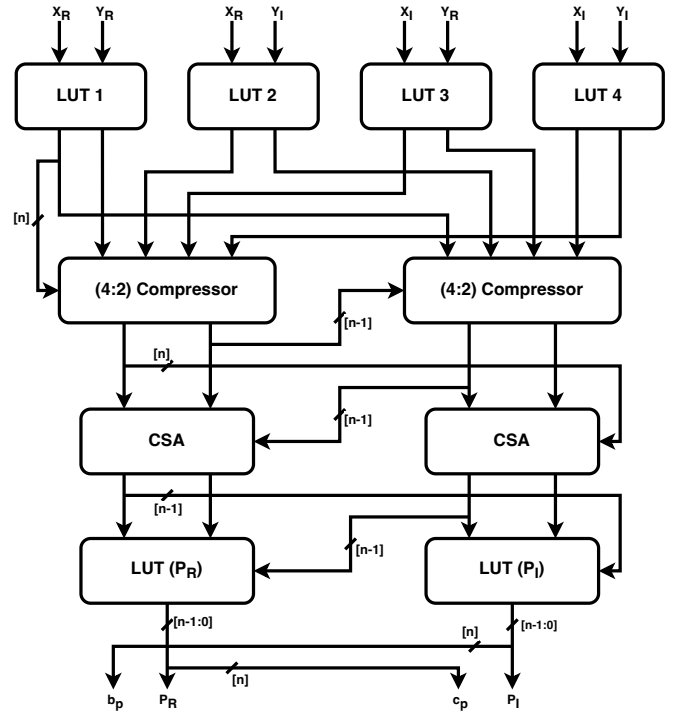


Fig. 2. Proposed complex-number modulo Multiplier diagram.

delay is imposed regarding the conversion of the two complex-number residues to modulo- $(2^{2n} + 1)$ one.

IV. EVALUATION AND COMPARISON

Realization of the proposed adders and multipliers on FPGAs represents a significant step towards validating their practical applicability and performance characteristics. This section delves into the implementation details of these arithmetic units and their implementation on the Spartan-7S100 FPGA platform using the Vivado FPGA synthesis tool. Through this FPGA realization, we aim to demonstrate the practical merits of the adders and multipliers, highlighting their suitability for high-performance computing applications that demand reliable and efficient arithmetic operations. To ensure a fair and objective comparison of the proposed adders and multipliers with existing solutions, all similar works have been implemented on the same platform. This uniformity in the implementation platform allows for a direct and equitable evaluation of each design's performance, resource utilization, and power efficiency. By adopting the Spartan-7S100 FPGA across all designs, we eliminate variables that could arise from differences in hardware capabilities, synthesis optimizations, or architectural efficiencies inherent to different FPGA models. This approach guarantees that the comparative analysis focuses solely on the merits of the design methodologies and the inherent efficiencies of the proposed arithmetic units.

Table II presents the delay, area, and power measures of the proposed moduli compared to the superseded modulo. As indicated in the table, both moduli- $(2^5 \pm j)$ adder and multiplier outperform the moduli- $(2^{10} + 1)$ counterparts re-

garding all the three figures of merit. However, concerning the multipliers' area measures, note that when comparing the area of two FPGA designs, it's important to consider not just the number of utilized LUTs, but also the inclusion of other generic components like digital signal processor (DSP) blocks. In this case, while the second design uses fewer LUTs, the engagement of a DSP block can significantly impact the overall area. The reason is that the FPGA DSP blocks are universal units designed for efficient arithmetic operations and typically exhibit resource consumption overhead in comparison to specialized units.

TABLE II
FIGURES OF MERIT FOR DOUBLE COMPLEX-NUMBER MODULI VERSUS THE EQUIVALENT DOUBLE BIT-WIDTH MODULO

Moduli	Adder				Multiplier		
	Delay (ns)	Area (LUT)	Power (μ W)	PDP	Delay (ns)	Area (LUT)	Power (μ W)
$2^5 \pm j$	9.562	32	14.162	135	20.402	428	14.586
$2^{10} + 1$	16.19	67	10.515	170	23.72	214+1*	15.789

* DSP.

To show the substantial features of the proposed complex-number modulo adders and multipliers for a range of bit-width values, we provide for the Figures 3 to 8. The six plots therein illustrate the delay, area consumption and power dissipation of the proposed designs and those of modulo- $(2^{2n} + 1)$, for $3 \leq n \leq 10$. These figures clearly demonstrate that the proposed moduli significantly outperform the counterpart in terms of delay, area, and power consumption.

Additionally, concerning the area measurements, for modulo- $(2^{2n} + 1)$ when $n \geq 5$ and for the proposed moduli- $(2^n \pm j)$ when $n \geq 9$, the area depicted in the figures has been converted to all LUTs based on the average size of Digital Signal Processors (DSPs) derived from the synthesis results. This conversion was performed solely for the purpose of comparison.

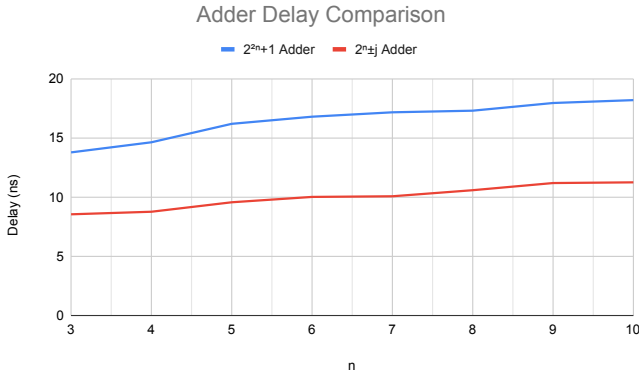


Fig. 3. Complex-number Modulo vs modulo- $(2^{2n} + 1)$ adder: Delay comparison.

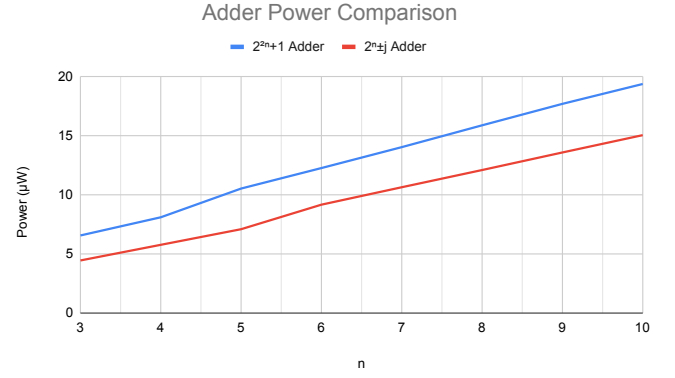


Fig. 4. Complex-number Modulo vs modulo- $(2^{2n} + 1)$ adder: Power comparison.

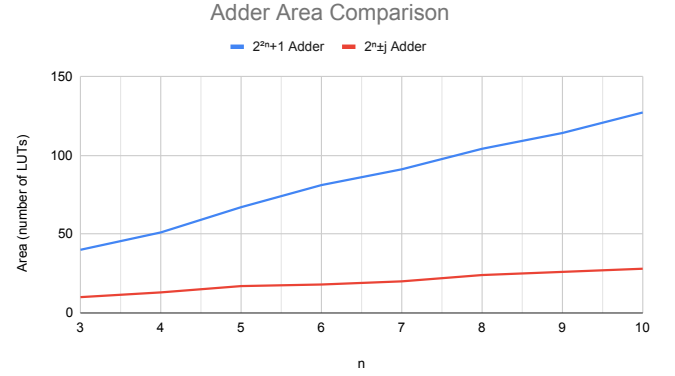


Fig. 5. Complex-number Modulo vs modulo- $(2^{2n} + 1)$ adder: Area comparison.

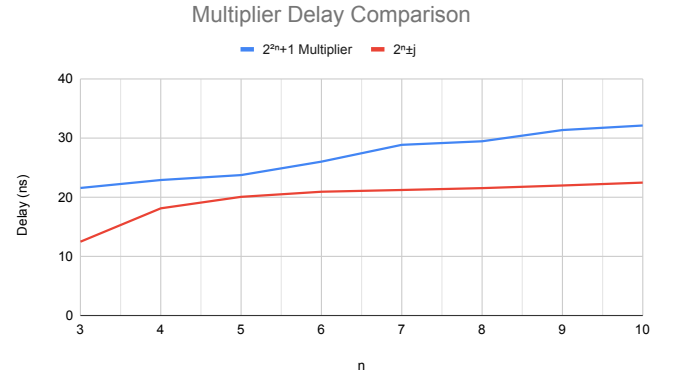


Fig. 6. Complex-number Modulo vs modulo- $(2^{2n} + 1)$ multiplier: Delay comparison.

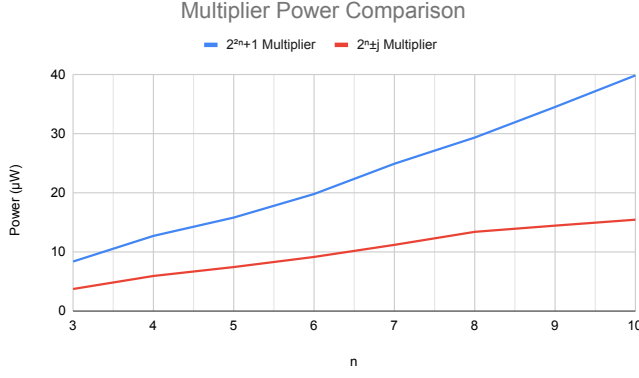


Fig. 7. Complex-number Modulo vs modulo- $(2^{2n} + 1)$ multiplier: Power comparison.

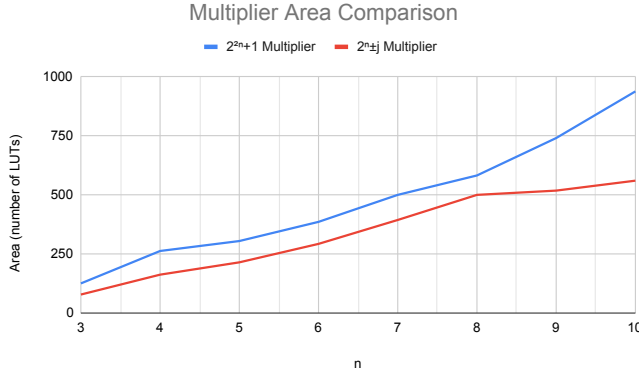


Fig. 8. Complex-number Modulo vs modulo- $(2^{2n} + 1)$ multiplier: Area comparison.

As anticipated, the synthesis results reveal that the slowest residue channel is attributed to modulo- $(2^n + 1)$. Tables III to VIII provide a comparison of the slowest channel delay, total area, and power consumption between the proposed replacement moduli-sets (RP1) and those utilized in previous RNS-DNN studies.

TABLE III
MODULI-SET REPLACEMENTS FOR RES-DNN [5], RNSIM [9], AND RNS-PM [16]

Moduli-Sets	Adder				
	Delay (ns)	Area (LUT)	Power (μ W)	PDP	DR
{31, 32, 63}	11.791	44	12.618	149	62,496
RP1: {7, 9, 16, $8 \mp j$ }	8.546	38	15.596	133	65,520
RP2: {15, 64, $8 \mp j$ }	8.851	34	14.312	127	62,400
Multiplier					
{31, 32, 63}	21.938	15.684	171	344	62,496
RP1: {7, 9, 16, $8 \mp j$ }	12.464	14.251	197	178	65,520
RP2: {15, 64, $8 \mp j$ }	12.464	15.793	220	197	62,400

TABLE IV
MODULI-SET REPLACEMENTS FOR RES-DNN [4]

Moduli-Sets	Adder				
	Delay (ns)	Area (LUT)	Power (μ W)	PDP	DR
{63, 64, 65}	13.777	73	15.934	220	262,080
RP1: {7, 9, 16, $8 \mp j$ }	8.763	44	18.238	160	259,056
RP2: {15, 128, $16 \mp j$ }	8.851	45	18.178	160	493,440
Multiplier					
{63, 64, 65}	21.938	239	19.452	427	262,080
RP1: {7, 9, 16, $8 \mp j$ }	18.102	365	18.653	338	259,056
RP2: {15, 128, $16 \mp j$ }	18.102	396	21.25	385	493,440

TABLE V
MODULI-SET REPLACEMENTS FOR RES-DNN [11]

Moduli-Sets	Adder				
	Delay (ns)	Area (LUT)	Power (μ W)	PDP	DR
{8, 63, 127}	11.803	56	14.661	173	64,008
RP1: {63, 65, 128, $64 \mp j$ }	8.546	38	15.596	133	65,520
RP2: {15, 128, $8 \mp j$ }	8.851	39	15.536	138	124,800
Multiplier					
{8, 63, 127}	22.135	211	16.32	361	64,008
RP1: {7, 9, 16, $8 \mp j$ }	12.464	134	13.022	162	65,520
RP2: {15, 128, $8 \mp j$ }	12.464	228	16.848	210	124,800

TABLE VI
MODULI-SET REPLACEMENTS FOR RES-DNN [12]

Moduli-Sets	Adder				
	Delay (ns)	Area (LUT)	Power (μ W)	PDP	DR
{3, 5, 7, 11, 13, 16, 17, 19, 23}	12.407	125	29.315	364	1,784,742,960
RP1: {63, 65, 128, $64 \mp j$ }	13.777	110	35.466	489	2,147,483,520
RP2: {15, 31, 1024, $64 \mp j$ }	10.015	72+1*	30.831	309	1,950,827,520
Multiplier					
{3, 5, 7, 11, 13, 16, 17, 19, 23}	24.845	348	34.232	850	1,784,742,960
RP1: {63, 65, 128, $64 \mp j$ }	21.938	831	38.781	851	2,147,483,520
RP2: {15, 31, 1024, $64 \mp j$ }	20.906	690+1*	36.625	766	1,950,827,520

* DSP.

TABLE VII
MODULI-SET REPLACEMENTS FOR RES-DNN [13]

Moduli-Sets	Adder				
	Delay (ns)	Area (LUT)	Power (μ W)	PDP	DR
L: {32, 31, 33, 29, 35}	15.297	131	24.156	370	33,227,040
RP1: {31, 32, 33, $32 \mp j$ }	12.65	88	26.487	335	33,554,400
RP2: {15, 31, 128, $32 \mp j$ }	9.562	64	24.503	234	61,008,000
H: {512, 511, 513}	14.894	107	24.074	359	134,217,216
RP1: {31, 32, 33, $64 \mp j$ }	12.65	92	30.633	388	134,119,392
RP2: {15, 31, 128, $64 \mp j$ }	10.015	69	28.649	287	243,853,440
Multiplier					
L: {32, 31, 33, 29, 35}	21.09	397	29.932	631	33,227,040
RP1: {31, 32, 33, $32 \mp j$ }	21.09	619	30.701	647	33,554,400
RP2: {15, 31, 128, $32 \mp j$ }	20.042	565	29.852	598	61,008,000
H: {512, 511, 513}	23.555	415+1*	31.863	751	134,217,216
RP1: {31, 32, 33, $64 \mp j$ }	21.09	775	34.119	720	134,119,392
RP2: {15, 31, 128, $64 \mp j$ }	20.906	721	33.27	696	243,853,440

* DSP.

TABLE VIII
MODULI-SET REPLACEMENTS FOR RES-DNN [17]

Moduli-Sets	Adder				
	Delay (ns)	Area (LUT)	Power (μ W)	PDP	DR
{31, 128, 511}	12.562	60	17.356	217	2,027,648
RP1: {15, 17, 32, $16 \mp j$ }	12.257	65	21.347	262	2,097,120
RP2: {15, 31, 32, $16 \mp j$ }	8.99	55	20.191	182	3,824,160
Multiplier					
{31, 128, 511}	23.126	279	21.822	505	2,027,648
RP1: {15, 17, 32, $16 \mp j$ }	18.102	441	24.505	444	2,097,120
RP2: {15, 31, 32, $16 \mp j$ }	18.559	430	21.633	401	3,824,160

Tables III to VIII illustrate that in certain instances, the area consumption of the proposed replacement moduli (RP1 and RP2) exceeds that of the reference counterparts. This

phenomenon may be attributed to the magnitude of n , as evidenced by the fact that increasing n leads to a more pronounced increase in the area of the proposed multiplier. With larger values of n , the synthesis tool faces challenges in optimizing the design, resulting in the dispersion of LUTs across the FPGA and consequently higher area utilization in terms of the LUT count. However, despite the increased area, the proposed moduli set consistently outperforms its predecessors in terms of delay and Power-Delay Product (PDP).

REFERENCES

- [1] Rei Ueno and Naofumi Homma. High-speed hardware architecture for post-quantum diffie-hellman key exchange based on residue number system. In *2022 IEEE International Symposium on Circuits and Systems (ISCAS)*, pages 2107–2111, 2022.
- [2] Ghassem Jaberipur and Bardia Nadimi. Balanced $(3+2\log n)\delta g$ adders for moduli set $\{2^{n+1}, 2^n + 2^{n-1} - 1, 2^{n+1} - 1\}$. *IEEE Transactions on Circuits and Systems I: Regular Papers*, 67(4):1368–1377, 2020.
- [3] Nikolai I. Chervyakov, Pavel A. Lyakhov, Nikolai N. Nagornov, Dmitrii I. Kaplun, Alexander S. Voznesenskiy, and Danil V. Bogayevskiy. Implementation of smoothing image filtering in the residue number system. In *2019 8th Mediterranean Conference on Embedded Computing (MECO)*, pages 1–4, 2019.
- [4] Sahand Salamat, Mohsen Imani, Sarangh Gupta, and Tajana Rosing. Rnsnet: In-memory neural network acceleration using residue number system. In *2018 IEEE International Conference on Rebooting Computing (ICRC)*, pages 1–12, 2018.
- [5] Nasim Samimi, Mehdi Kamal, Ali Afzali-Kusha, and Massoud Pedram. Res-dnn: A residue number system-based dnn accelerator unit. *IEEE Transactions on Circuits and Systems I: Regular Papers*, 67(2):658–671, 2020.
- [6] Zhi-Gang Liu and Matthew Mattina. Efficient residue number system based winograd convolution. In Andrea Vedaldi, Horst Bischof, Thomas Brox, and Jan-Michael Frahm, editors, *Computer Vision – ECCV 2020*, pages 53–68, Cham, 2020. Springer International Publishing.
- [7] Vasilis Sakellariou, Vassilis Paliouras, Ioannis Kouretas, Hani Saleh, and Thanos Stouraitis. On reducing the number of multiplications in rns-based cnn accelerators. In *2021 28th IEEE International Conference on Electronics, Circuits, and Systems (ICECS)*, pages 1–6, 2021.
- [8] Maria Valueva, Georgii Valuev, Mikhail Babenko, Andrei Tchernykh, and Jorge M. Cortes-Mendoza. Method for convolutional neural network hardware implementation based on a residue number system. In *Programming and Computer Software*, volume 48, page 735–744, 2022.
- [9] Arman Roohi, MohammadReza Taheri, Shaahin Angizi, and Deliang Fan. Rnsim: Efficient deep neural network accelerator using residue number systems. In *2021 IEEE/ACM International Conference On Computer Aided Design (ICCAD)*, pages 1–9, 2021.
- [10] Sahand Salamat, Sumiran Shubhi, Behnam Khaleghi, and Tajana Rosing. Residue-net: Multiplication-free neural network by in-situ no-loss migration to residue number systems. In *2021 26th Asia and South Pacific Design Automation Conference (ASP-DAC)*, pages 222–228, 2021.
- [11] Valentina Arrigoni, Beatrice Rossi, Pasqualina Fragneto, and Giuseppe S. Desoli. Approximate operations in convolutional neural networks with rns data representation. In *The European Symposium on Artificial Neural Networks*, 2017.
- [12] Hiroki Nakahara and Tsutomu Sasao. A high-speed low-power deep neural network on an fpga based on the nested rns: Applied to an object detector. In *2018 IEEE International Symposium on Circuits and Systems (ISCAS)*, pages 1–5, 2018.
- [13] Wan-Ju Huang, Hsiao-Wen Fu, and Tsung-Chu Huang. An-hrns: An-coded hierarchical residue number system for reliable neural network accelerators. In *2022 IEEE 31st Asian Test Symposium (ATS)*, pages 132–137, 2022.
- [14] Xilinx. Sp701 evaluation kit board user guide (document no. ug1319). Retrieved from [https://www.xilinx.com/support/documents/boards_and_kits/sp701/ug1319-sp701-eval-bd.pdf], 2019.
- [15] Yuke Wang. Residue-to-binary converters based on new chinese remainder theorems. *IEEE Transactions on Circuits and Systems II: Analog and Digital Signal Processing*, 47(3):197–205, 2000.
- [16] Shaahin Angizi, Arman Roohi, MohammadReza Taheri, and Deliang Fan. Processing-in-memory acceleration of mac-based applications using residue number system: A comparative study. In *Proceedings of the 2021 on Great Lakes Symposium on VLSI, GLSVLSI '21*, page 265–270, New York, NY, USA, 2021. Association for Computing Machinery.
- [17] Nikolai I. Chervyakov, Pavel A. Lyakhov, Maxim A. Deryabin, Nikolay N. Nagornov, Maria V. Valueva, and Georgii V. Valuev. Residue number system-based solution for reducing the hardware cost of a convolutional neural network. *Neurocomputing*, 407:439–453, 2020.
- [18] Chingyu Hung and Behrooz. Parhami. An approximate sign detection method for residue numbers and its application to rns division. *Computers & Mathematics with Applications*, 27(4):23–35, 1994.

Appendix:

(F -to-modulo- $(2^{2n} + 1)$ conversion): Let $Z = 2^{4n}Z_2 + 2^{2n}Z_1 + Z_0$, represents the $5n$ -bit numbers within the dynamic range of F , where $Z_2 = z_{5n-1} \cdots z_{4n} \in [0, 2^n - 1]$, $Z_1 = z_{4n-1} \cdots z_{2n} \in [0, 2^{2n} - 1]$, and $Z_0 = z_{2n-1} \cdots z_0 \in [0, 2^{2n} - 1]$. We obtain $X = |Z|_{2^{2n}+1}$, as follows.

$$X = |Z|_{2^{2n}+1} = |2^{4n}Z_2 + 2^{2n}Z_1 + Z_0|_{2^{2n}+1} = |Z_2 - Z_1 + Z_0|_{2^{2n}+1} = |Z_2 + \overline{Z_1} - 2^{2n} + 1 + Z_0|_{2^{2n}+1} = |Z_2 + \overline{Z_1} + Z_0 + 2|_{2^{2n}+1}.$$
Let $U = u_{2n-1} \cdots u_0$, and $V = v_{2n-1} \cdots v_1 \overline{v_{2n}}$, be obtained, via a modulo- $(2^{2n} + 1)$ carry-save adder operating on $|Z_2 + \overline{Z_1} + Z_0 + 1|_{2^{2n}+1}$. Therefore, $X = |Z_2 + \overline{Z_1} + Z_0 + 2|_{2^{2n}+1} = |U + V + 1|_{2^{2n}+1} = |x_{2n}x_{2n-1} \cdots x_0 + 1|_{2^{2q}+1}$, where $|U + V|_{2^{2n}+1}$ is assumed to yield $x_{2n}x_{2n-1} \cdots x_0 \in [0, 2^{2n}]$, via a modulo- $(2^{2n} + 1)$ adder. Finally, $X = |x_{2n}x_{2n-1} \cdots x_0 + 1|_{2^{2q}+1} = |x_{2n-1} \cdots x_0 + 1 - x_{2n}|_{2^{2q}+1} = x_{2n-1} \cdots x_0 + \overline{x_{2n}} \in [0, 2^{2n}]$, where $x_{2n} = 1 \rightarrow x_{2n-1} \cdots x_0 = 0$.